Chapter 1

Exceptional Points

Denis V. Novitsky[a] and Andrey V. Novitsky[b,c]

[a]B. I. Stepanov Institute of Physics, National Academy of Sciences of Belarus, Nezavisimosti Avenue 68, 220072 Minsk, Belarus, [b]Department of Theoretical Physics and Astrophysics, Belarusian State University, Nezavisimosti Avenue 4, 220030 Minsk, Belarus, [c]ITMO University, Kronverksky Prospekt 49, 197101 St. Petersburg, Russia

ABSTRACT

This Chapter overviews the physics of non-Hermitian degeneracies at the so-called exceptional points. We consequentially give an introduction to theoretical aspects of non-Hermitian physics and fundamentals of exceptional points supporting our conclusions with specific examples borrowed from optics and photonics studies. In particular, we consider exceptional points on the ground of both passive components and active media containing loss and gain. In the latter case, the optical $\mathcal{PT}$ symmetry, an especially fruitful notion, is feasible. Exceptional points in $\mathcal{PT}$-symmetric systems can be also defined as a border between symmetric and symmetry-broken phases. The Chapter embraces discussion of topological properties of exceptional points observed under static and dynamic encircling and the basics of enhanced sensing near exceptional points able to detect single molecules. Finally, we show that the exceptional points are useful for studying the strong light-matter coupling in polariton physics.

KEYWORDS

Non-Hermitian photonics, Exceptional point, $\mathcal{PT}$ symmetry, Lasing, Optical sensing, Topological charge, Strong coupling

1.1 INTRODUCTION

Among the recent trends in optical science, non-Hermitian photonics seems to be one of the most intriguing and promising. Generally speaking, it considers interaction of photonic structures as open dynamic systems with light. This approach allows one to look at the problem of light-matter interaction from another angle providing a different treatment even for well-known optical systems, such as lasers and coupled resonators. On the other hand, the non-Hermitian photonics has put forward the structures (for example, $\mathcal{PT}$-symmetric ones) that were not even imagined before. As a result, a number of unusual, entirely unexpected features and effects due to the non-Hermiticity of photonic structures has been predicted and experimentally observed.

Non-Hermitian matrices describing Hamiltonians and scattering operators are in the heart of the non-Hermitian physics. They admit a distinctive type of

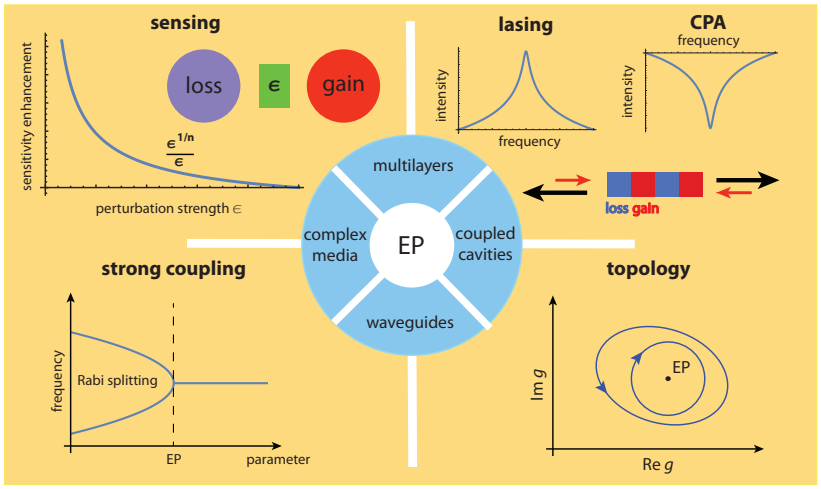

FIGURE 1.1 Roadmap on exceptional points (EP) within this Chapter. Inner blue ring demonstrates four types of systems often used for investigation of EPs. In the Chapter, we discuss the EP-based sensors, lasers and coherent perfect absorbers (CPA), as well as perspectives of the EPs for polaritonic physics and topology.

degeneracy at the exceptional point (EP) when both eigenvalues and eigenvectors coalesce, so that the set of eigenfunctions becomes defective. It should be stressed that this type of degeneracy is impossible in the Hermitian case. The principles of non-Hermitian physics and exceptional points as their manifestation proved to be fruitful in various branches of classical and quantum physics including optics, acoustics, mechanics, electronics, and even biophysics [1].

In this Chapter, we start with the basic theoretical premises for the EPs, describe their properties, and then illustrate them with the examples of EPs in nanophotonics. In particular, we demonstrate the appearance of EPs in passive systems with purely radiative losses and in structures with spatially distributed gain and loss including $\mathcal{PT}$-symmetric ones. We discuss topological properties of EPs, their application for sensing, and connection with the strong-coupling physics (Fig. 1.1). There is a number of books [2–4] and review articles [5–8] on non-Hermitian physics and its application to photonics, while different aspects of EPs are discussed in [9,10]. We do not aim to compete with this literature in completeness and breadth of coverage. Instead, we try to make a general educational introduction to the subject of EPs for the dielectric photonics community and, especially, for beginners in non-Hermitian photonics. A reader interested in more details and examples may consult references herein.

1.2 GENERAL THEORY OF EXCEPTIONAL POINTS

1.2.1 The eigenvalue problem

Many physical systems are governed by a set of linear differential equations of the first order in the form of the non-stationary Schrödinger equation

$$i\frac{d\psi}{d\tau} = \hat{H}(\vec{\alpha})\psi, \tag{1.1}$$

where τ is the evolution variable (either time or coordinate), $\psi(\tau, \vec{\alpha})$ and $\hat{H}(\vec{\alpha})$ are n-dimensional vector (wave function) and matrix (Hamiltonian), respectively, and $\vec{\alpha} = (\alpha_1, \ldots, \alpha_m)$ is a vector of m parameters. Here we assume that the Hamiltonian $\hat{H}$ can be either Hermitian ($\hat{H} = \hat{H}^\dagger$, where the superscript $\dagger$ stands for the Hermitian conjugate) as in quantum mechanics or non-Hermitian ($\hat{H} \neq \hat{H}^\dagger$). Equation (1.1) emerges in many areas of physics spanning quantum mechanics, acoustics, photonics, and classical electrodynamics. The simplest type of a system obeying Eq. (1.1) is the two-state one. It is described by the 2×2 Hamiltonian as follows

$$i\frac{d}{d\tau}\begin{pmatrix} \psi_1 \\ \psi_2 \end{pmatrix} = \begin{pmatrix} H_{11} & H_{12} \\ H_{21} & H_{22} \end{pmatrix}\begin{pmatrix} \psi_1 \\ \psi_2 \end{pmatrix}. \tag{1.2}$$

Such an equation describes evolution of two coupled optical or acoustic modes with the diagonal elements of the Hamiltonian corresponding to the complex resonant frequencies and the non-diagonal elements representing coupling strength between the modes. Generalization of Eq. (1.2) to higher dimensions is straightforward.

In electrodynamics of complex media, the propagation of stationary electromagnetic waves can be often considered in one dimension and described by the four-dimensional vector comprising independent transverse field components $\mathbf{H}_t$ and $\mathbf{E}_t$ as

$$\frac{d}{dz}\begin{pmatrix} \mathbf{H}_t \\ \mathbf{E}_t \end{pmatrix} = i\frac{\omega}{c}\begin{pmatrix} M_{11} & M_{12} \\ M_{21} & M_{22} \end{pmatrix}\begin{pmatrix} \mathbf{H}_t \\ \mathbf{E}_t \end{pmatrix}, \tag{1.3}$$

where M_{ij} are the 2×2 block matrices depending on material parameters, ω is the angular frequency and c is the speed of light in vacuum.

Fundamental solution of Eq. (1.1) can be formally written as

$$\psi(\tau, \vec{\alpha}) = \exp[-i\hat{H}(\vec{\alpha})\tau]\psi(0, \vec{\alpha}). \tag{1.4}$$

Here exponential of matrix $\hat{H}$ is defined through a corresponding Taylor series. The Hamiltonian matrix can be spectrally decomposed,

$$\hat{H} = \sum_{j=1}^{n} \lambda_j \hat{P}_j, \tag{1.5}$$

where λ_j are the eigenvalues of $\hat{H}$ forming its spectrum and $\hat{P}_j = \mathbf{v}_j \otimes \mathbf{u}_j$ are the projectors onto the corresponding eigenvectors with the property $\hat{P}_j^2 = \hat{P}_j$. The tensor product of two vectors $\mathbf{u}$ and $\mathbf{v}$ is defined as a matrix $n \times n$ with elements $(\mathbf{u} \otimes \mathbf{v})_{jk} = u_j v_k$, where $j, k = 1, \ldots n$. Right $\mathbf{v}_j$ and left $\mathbf{u}_j$ eigenvectors are defined in accordance with

$$\hat{H}\mathbf{v}_j = \lambda_j \mathbf{v}_j, \qquad \mathbf{u}_j \hat{H} = \lambda_j \mathbf{u}_j \tag{1.6}$$

and satisfy the orthonormality condition $\mathbf{u}_j \mathbf{v}_k = \delta_{jk}$ providing orthogonality of the projectors $\hat{P}_j \hat{P}_k = \hat{P}_j \delta_{jk}$. Here δ_{jk} is the Kronecker delta defined as usual: $\delta_{jk} = 1$ for $j = k$ and $\delta_{jk} = 0$ for $j \neq k$. If the matrix is symmetric, $\hat{H} = \hat{H}^T$, then the right and left eigenvectors coincide, $\mathbf{v}_j = \mathbf{u}_j^T$, where the superscript T stands for the transpose.

Eigenvalues λ meet the characteristic equation $\det(\hat{H} - \lambda I_n) = 0$ and can be written by means of n matrix invariants, e.g., the traces of matrix powers $\mathrm{tr}(\hat{H}) = \sum_{j=1}^n \lambda_j$, $\ldots$, $\mathrm{tr}(\hat{H}^{n-1}) = \sum_{j=1}^n \lambda_j^{n-1}$ and the determinant $\det(\hat{H}) = \lambda_1 \ldots \lambda_n$, where I_n is the $n \times n$ unit matrix. The projectors can be determined from the system of n equations including the completeness condition $I_n = \sum_{j=1}^n \hat{P}_j$ and the condition for the Hamiltonian powers: $\hat{H} = \sum_{j=1}^n \lambda_j \hat{P}_j$, $\ldots$, $\hat{H}^{n-1} = \sum_{j=1}^n \lambda_j^{n-1} \hat{P}_j$.

Using the spectral decomposition, we arrive at the fundamental solution (1.4) in the following form

$$\psi(\tau, \vec{\alpha}) = \sum_{j=1}^{n} \exp[-i\lambda_j(\vec{\alpha})\tau] \hat{P}_j(\vec{\alpha}) \psi(0, \vec{\alpha}). \tag{1.7}$$

The spectral decomposition can be used for solving the Schrödinger differential equation with a source $\mathbf{J}$, e.g., a dipole. For the stationary wave function ψ and the source $\mathbf{J}$ proportional to $\exp(-i\lambda\tau)$, this equation reads

$$\hat{H}\psi + \mathbf{J} = \lambda\psi. \tag{1.8}$$

Substituting decomposition $\psi = \sum_m a_m \mathbf{v}_m$ into the above equation and accounting for $\hat{H}\mathbf{v}_m = \lambda_m \mathbf{v}_m$, we arrive at the equation for a_m: $\sum_m a_m(\lambda - \lambda_m)\mathbf{v}_m = \mathbf{J}$. The wave function takes the form

$$\psi = G\mathbf{J}, \qquad G = \sum_m \frac{1}{\lambda - \lambda_m} \frac{\mathbf{v}_m \otimes \mathbf{u}_m}{(\mathbf{u}_m \mathbf{v}_m)}. \tag{1.9}$$

Here G is the dyadic Green function.

1.2.2 Definition of exceptional points

When we change the parameters $\vec{\alpha}$, some eigenvalues may turn out to be equal. Generally we can have M sets of equal eigenvalues as $\lambda_1 = \ldots = \lambda_{n_1} = \tilde{\lambda}_1$,

$\lambda_{n_1+1} = \ldots = \lambda_{n_2} = \tilde{\lambda}_2, \ldots \lambda_{n_{M-1}} = \ldots = \lambda_n = \tilde{\lambda}_M$. A unique eigenvalue $\tilde{\lambda}$ corresponds to a block in the matrix $\hat{H}$. It is instructive to focus further on the Hamiltonian possessing a single degenerate eigenvalue.

Assume that the eigenvalues of the n-dimensional matrix $\hat{H}$ at the point $\vec{\alpha}_0$ in the parameter space $(\alpha_1, \ldots, \alpha_m)$ are equal, $\lambda_1 = \ldots = \lambda_n = \lambda$. Depending on the Hamiltonian Hermiticity, the point $\vec{\alpha}_0$ is called either diabolic or exceptional.

(i) At the *diabolic point*, the matrix $\hat{H}$ is diagonalizable, so that it can be represented as

$$\hat{H}(\vec{\alpha}_0) = h\hat{I}_n. \tag{1.10}$$

The degenerate eigenvalues $\lambda = h$ correspond to the orthogonal eigenvectors and the fundamental solution $\psi(\tau, \vec{\alpha}_0) = \exp(\lambda\tau)\psi(0, \vec{\alpha}_0)$ is trivial.

(ii) At the *exceptional point*, the matrix is non-diagonalizable, so that

$$\hat{H}(\vec{\alpha}_0) = h\hat{I}_n + \hat{N}, \tag{1.11}$$

where $\hat{N}$ is a nilpotent matrix defined as $\hat{N}^n = 0$ with $\hat{N}^j \neq 0$ for $j < n$. Adding the nilpotent matrix to the diagonal one does not affect the degenerate eigenvalue $\lambda = h$, but drastically influences the eigenvectors. As well as the eigenvalues, the eigenvectors at the EP are degenerate, i.e., there is a single eigenvector at the EP satisfying the equation $\hat{H}\mathbf{v}_1 = \lambda\mathbf{v}_1$, the left eigenvector being orthogonal to it as $\mathbf{u}_1\mathbf{v}_1 = 0$. As a result, the basis set of orthogonal eigenvectors cannot be established, but one can introduce the set of non-orthogonal *generalized eigenvectors* using the following procedure. Equation for the degenerate eigenvector $(\hat{H} - \lambda)\mathbf{v}_1 = 0$ can be rewritten as $\hat{N}\mathbf{v}_1 = 0$ after substitution of Eq. (1.11). Generalized eigenvectors do not meet this equation, that is $\hat{N}\mathbf{v}_2 \neq 0$. Instead, the first generalized eigenvector satisfies equation

$$\hat{N}\mathbf{v}_2 = \mathbf{v}_1, \qquad \text{or} \qquad (\hat{H} - \lambda)\mathbf{v}_2 = \mathbf{v}_1. \tag{1.12}$$

After multiplying both sides of this equation by the nilpotent matrix $\hat{N}$, we obtain $\hat{N}^2\mathbf{v}_2 = 0$ or $(\hat{H} - \lambda)^2\mathbf{v}_2 = 0$. The second generalized eigenvector is defined in the similar manner as

$$\hat{N}\mathbf{v}_3 = \mathbf{v}_2, \qquad \text{or} \qquad (\hat{H} - \lambda)\mathbf{v}_3 = \mathbf{v}_2. \tag{1.13}$$

Multiplication by the matrix $\hat{N}^2$ yields $\hat{N}^3\mathbf{v}_2 = 0$ or $(\hat{H} - \lambda)^3\mathbf{v}_2 = 0$. Thus, the generalized eigenvectors are defined by the chain rule $\hat{N}\mathbf{v}_j = \mathbf{v}_{j-1}$, where $j = 2, \ldots, n$. This chain rule allows us to determine the form of the nilpotent matrix $\hat{N}$. It is quite easy to notice that the chain rule is valid, if

$$\hat{N} = \sum_{j=1}^{n-1} \mathbf{v}_j \otimes \mathbf{u}_{n-j}, \tag{1.14}$$

where $\mathbf{u}_{n-j}\mathbf{v}_k = \delta_{j,k-1}$ or $\mathbf{u}_j\mathbf{v}_k = \delta_{n-j,k-1}$. Generalized left eigenvectors $\mathbf{u}_j$ can be found from the chain rule $\mathbf{u}_j\hat{N} = \mathbf{u}_{j-1}$ $(j = 2, \ldots, n)$ consistent with the

dyadic decomposition (1.14) of $\hat{N}$. The degenerate left eigenvector meets the equation $\mathbf{u}_1\hat{N} = 0$.

The Hamiltonian matrix can be presented in the Jordan canonical form assuming non-zero elements on the superdiagonal $(k, k+1)$ of the nilpotent matrix $(k = 1, \ldots, n-1)$ as follows

$$\hat{H}(\vec{\alpha}_0) = \begin{pmatrix} \lambda & 1 & 0 & 0 & 0 & \ldots \\ 0 & \lambda & 1 & 0 & 0 & \ldots \\ 0 & 0 & \lambda & 1 & 0 & \ldots \\ \ldots & \ldots & \ldots & \ldots & \ldots & \ldots \end{pmatrix}. \tag{1.15}$$

In order to obtain other forms of the Hamiltonian matrix at the EP, one should exploit a similarity transformation S in the n-dimensional space. Then the Hamiltonian reads $\hat{H}'(\vec{\alpha}_0) = \hat{S}(h\hat{I}_n + \hat{N})\hat{S}^{-1} = h\hat{I}_n + \hat{N}'$, where $\hat{N}' = \hat{S}\hat{N}\hat{S}^{-1}$.

At the EP, the fundamental solution (1.4) of differential equations (1.1) reads

$$\psi(\tau, \vec{\alpha}_0) = \exp(-i\lambda\tau)\exp(-i\hat{N}\tau)\psi(0, \vec{\alpha}_0). \tag{1.16}$$

Exponential of the nilpotent matrix is defined as a truncated Taylor series due to $\hat{N}^k = 0$ for $k \geq n$. Therefore, we get

$$\psi(\tau, \vec{\alpha}_0) = \exp(-i\lambda\tau)\left[\sum_{k=0}^{n-1} \frac{(-i\tau)^k}{k!}\hat{N}^k\right]\psi(0, \vec{\alpha}_0). \tag{1.17}$$

This means that the solution is not just an exponential at the EP. Using decomposition over the basis of generalized eigenvectors for the initial wave function $\psi(0, \vec{\alpha}_0) = \sum_{j=1}^{n} c_j\mathbf{v}_j$, we can notice that the action of the nilpotent matrix reduces to $\hat{N}\psi(0, \vec{\alpha}_0) = \sum_{j=2}^{n} c_j\mathbf{v}_{j-1} = \sum_{j=1}^{n-1} c_{j+1}\mathbf{v}_j$ and the solution (1.17) reads

$$\psi(\tau, \vec{\alpha}_0) = \exp(-i\lambda\tau)\sum_{k=0}^{n-1} \frac{(-i\tau)^k}{k!}\sum_{j=1}^{n-k} c_{j+k}\mathbf{v}_j. \tag{1.18}$$

The EPs are known to exist for electromagnetic waves in (bi)anisotropic crystals, which evolution is described with 4×4 Jordan matrices as in Eq. (1.3). Since the nilpotent matrix is 4-dimensional, one is able to distinguish waves with exponential-linear (Voigt waves), exponential-quadratic and exponential-cubic dependence on the coordinate instead of regular plane-wave solutions [11]. Recently, it was introduced a concept of Dyakonov-Voigt surface waves propagating only in certain directions at the interface of anisotropic medium and decaying away from the interface as a product of linear and exponential functions [12].

Hermitian Hamiltonians with degenerate spectrum can support only diabolic points, so that the set of orthogonal eigenvectors can be always found. Since the Hamiltonian at the EP (1.15) is clearly non-Hermitian, the EPs emerge exclusively for non-Hermitian Hamiltonians. Although non-Hermiticity can be

arbitrary, the most curious cases correspond to certain symmetries, for example, $\mathcal{PT}$ and anti-$\mathcal{PT}$ symmetries as it will be discussed further.

The Green function at the exceptional point λ_{EP} can be found as follows (see [13,14]). Subtracting the term $\lambda_{EP}\psi$ from the left and right hand sides of Eq. (1.8), we write

$$(\hat{H}_0 - \lambda_{EP} I_n)\psi + \mathbf{J} = (\lambda - \lambda_{EP})\psi \tag{1.19}$$

or

$$\psi = \frac{1}{\lambda - \lambda_{EP}} \left(I_n - \frac{\hat{N}}{\lambda - \lambda_{EP}} \right)^{-1} \mathbf{J}. \tag{1.20}$$

Exploiting the Taylor series of this matrix function, the Green function defined as $\psi = G_{EP}\mathbf{J}$ can be presented in the form

$$G_{EP} = \frac{1}{\lambda - \lambda_{EP}} \sum_{k=0}^{\infty} \frac{\hat{N}^k}{(\lambda - \lambda_{EP})^k}. \tag{1.21}$$

The series is truncated due to the property of the nilpotent matrix $\hat{N}^n = 0$ yielding

$$G_{EP} = \frac{1}{\lambda - \lambda_{EP}} \sum_{k=0}^{n-1} \frac{\hat{N}^k}{(\lambda - \lambda_{EP})^k} = \frac{I_n}{\lambda - \lambda_{EP}} + \frac{\hat{N}}{(\lambda - \lambda_{EP})^2} + \ldots + \frac{\hat{N}^{n-1}}{(\lambda - \lambda_{EP})^n}. \tag{1.22}$$

Note that the leading-order term of the Green function at the EP is the last one, proportional to $(\lambda - \lambda_{EP})^{-n}$, if λ is close to λ_{EP}.

1.2.3 Exceptional points of two-state Hamiltonians

Consider a non-Hermitian Hamiltonian $\hat{H}(\vec{\alpha})$ that can be described by the 2×2 matrix. It governs evolution of the system given by Eq. (1.2) with the fundamental solution (1.4). Spectrum of the Hamiltonian $\hat{H}$ consists of a couple of eigenvalues λ_1 and λ_2 and the Hamiltonian can be presented as $\hat{H} = \lambda_1\hat{P}_1 + \lambda_2\hat{P}_2$ with the projectors $\hat{P}_1$ and $\hat{P}_2$. The eigenvalues can be written by means of the matrix invariants $\mathrm{tr}(\hat{H}) = \lambda_1 + \lambda_2$ and $\det(\hat{H}) = \lambda_1\lambda_2$ as

$$\lambda_{1,2} = \frac{\mathrm{tr}(\hat{H}) \pm \sqrt{[\mathrm{tr}(\hat{H})]^2 - 4\det(\hat{H})}}{2}. \tag{1.23}$$

The equations $\hat{P}_1 + \hat{P}_2 = \hat{I}_2$ and $\lambda_1\hat{P}_1 + \lambda_2\hat{P}_2 = \hat{H}$ yield the projecting matrices

$$\hat{P}_1 = \frac{1}{\lambda_1 - \lambda_2} \left(\hat{H} - \lambda_2 \hat{I}_2 \right), \qquad \hat{P}_2 = \frac{1}{\lambda_2 - \lambda_1} \left(\hat{H} - \lambda_1 \hat{I}_2 \right). \tag{1.24}$$

At the point $\vec{\alpha}_0$ of the parameter space, where the square root in Eq. (1.23) vanishes, the eigenvalues coalesce, $\lambda = \lambda_1 = \lambda_2 = \mathrm{tr}(\hat{H})/2$. If the eigenvectors also coalesce at this point, we have the EP of the second order. The eigenvalues

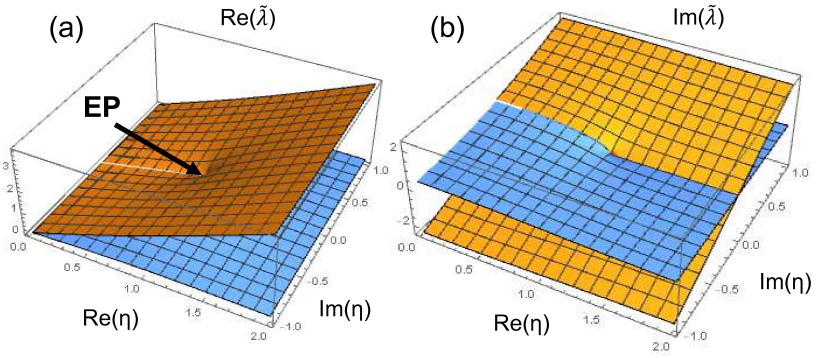

FIGURE 1.2 The EP of a two-state Hamiltonian. The real (a) and imaginary (b) parts of the normalized eigenvalues (1.23), $\lambda_{1,2}/\sqrt{\det(\hat{H})}$, as a function of complex parameter $\eta = \mathrm{tr}(\hat{H})/2\sqrt{\det(\hat{H})}$. The EP is observed at $\mathrm{Re}(\eta) = 1$ and $\mathrm{Im}(\eta) = 0$.

of a generic two-dimensional system are shown in Fig. 1.2. One can see that in order to reach the EP, one has to tune two parameters – the real and imaginary parts of the value $\eta = \mathrm{tr}(\hat{H})/2\sqrt{\det(\hat{H})}$.

In the case of real-valued $\mathrm{tr}(\hat{H})$ and $\det(\hat{H})$, the eigenvalues are real at the EP independent of Hermiticity. The EP then lies on the line $[\mathrm{tr}(\hat{H})]^2 = 4\det(\hat{H})$ separating two phases, the first one being symmetric ($[\mathrm{tr}(\hat{H})]^2 > 4\det(\hat{H})$), while the second one being symmetry-broken ($[\mathrm{tr}(\hat{H})]^2 < 4\det(\hat{H})$). There is a single real-valued parameter η to be tuned as shown Fig. 1.3. In the symmetric phase of the non-Hermitian Hamiltonian, the evolution of the system resembles that of a Hermitian system characterized by real eigenvalues. Symmetric phase requires symmetry of the non-Hermitian Hamiltonian and, hence, of the system itself. In the symmetry-broken phase, the eigenvalues are the complex-conjugate pair corresponding to the amplifying and decaying solutions. For the complex invariants $\mathrm{tr}(\hat{H})$ and $\det(\hat{H})$, the eigenvalues are complex in both phases, but the Hamiltonian matrix still has the Jordan form at the EP, when $[\mathrm{tr}(\hat{H})]^2 = 4\det(\hat{H})$.

At the EP, the Hamiltonian may be written in the canonical Jordan form

$$\hat{H}(\vec{\alpha}_0) = \lambda\hat{I}_2 + \hat{N} = \begin{pmatrix} \lambda & 1 \\ 0 & \lambda \end{pmatrix}, \tag{1.25}$$

The two-dimensional nilpotent matrix satisfies $\hat{N}^2 = 0$. Using the similarity transformation $\hat{S} = \mathrm{diag}(s_1, s_2)$, we can present the nilpotent matrix as $\hat{N}' = \hat{S}\hat{N}\hat{S}^{-1} = (s_1/s_2)\hat{N}$. Using an orthogonal matrix $\hat{S}(\alpha) = \begin{pmatrix} \cos\alpha & \sin\alpha \\ -\sin\alpha & \cos\alpha \end{pmatrix}$ to transform the nilpotent matrix yields a wide class of non-Hermitian Hamiltoni-

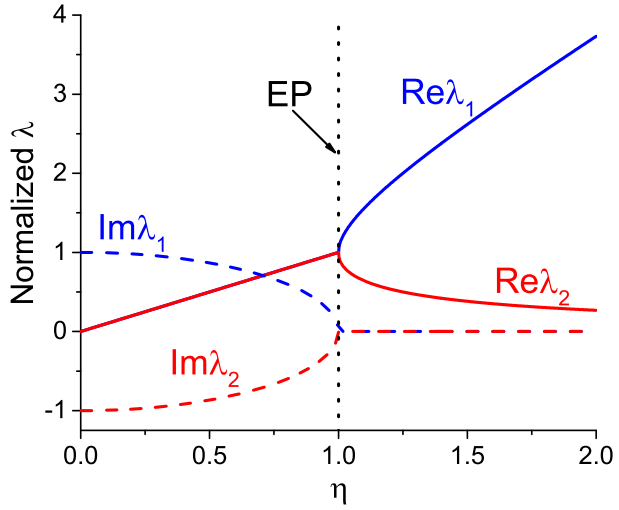

FIGURE 1.3 The EP of a two-state Hamiltonian. The normalized eigenvalues (1.23), $\lambda_{1,2}/\sqrt{\det(\hat{H})}$, as a function of real-valued $\eta = \mathrm{tr}(\hat{H})/2\sqrt{\det(\hat{H})}$. The EP is observed at $\eta = 1$.

ans, which at the EP has the form

$$\hat{H}(\vec{\alpha}_0) = \lambda \hat{I}_2 + \hat{S}(\alpha)\hat{N}\hat{S}^{-1}(\alpha) = \begin{pmatrix} \lambda + \sin\alpha\cos\alpha & \cos^2\alpha \\ -\sin^2\alpha & \lambda - \sin\alpha\cos\alpha \end{pmatrix}. \quad (1.26)$$

When $\alpha = i\beta$, the Hamiltonian at the EP is

$$\hat{H}(\vec{\alpha}_0) = \begin{pmatrix} \lambda + i\sinh\beta\cosh\beta & \cosh^2\beta \\ \sinh^2\beta & 1 - i\sinh\beta\cosh\beta \end{pmatrix}, \quad (1.27)$$

being a symmetric matrix, when $\cosh\beta = \sinh\beta$. The fundamental solution (1.17) at the EP can be written for any Hamiltonian we mentioned before. In the case of Hamiltonian (1.25), the fundamental solution at the EP reads

$$\begin{pmatrix} \psi_1(\tau) \\ \psi_2(\tau) \end{pmatrix} = e^{-i\lambda\tau}\begin{pmatrix} 1 & -i\tau \\ 0 & 1 \end{pmatrix}\begin{pmatrix} \psi_1(0) \\ \psi_2(0) \end{pmatrix} = e^{-i\lambda\tau}\begin{pmatrix} \psi_1(0) - i\tau\psi_2(0) \\ \psi_2(0) \end{pmatrix}. \quad (1.28)$$

Now we determine the generalized eigenvectors of the Hamiltonian (1.25). In the case of two coalescing eigenvectors, $n = 2$ and the nilpotent matrix $\hat{N} = \mathbf{v}_1 \otimes \mathbf{u}_1$ defined by Eq. (1.14) is a dyad. The normal right eigenvector $\mathbf{v}_1 = (1, 0)^T$ follows from the equation $(\hat{H} - \lambda\hat{I}_2)\mathbf{v}_1 = 0$. Single generalized eigenvector $\mathbf{v}_2 = (a_2, b_2)^T$ for the 2×2 Hamiltonian satisfies equation

$$\begin{pmatrix} 0 & 1 \\ 0 & 0 \end{pmatrix}\begin{pmatrix} a_2 \\ b_2 \end{pmatrix} = \begin{pmatrix} 1 \\ 0 \end{pmatrix}, \quad (1.29)$$

yielding $\mathbf{v}_2 = (w, 1)^T$, where w is a constant that can be found from a normalization condition. Similarly, we can determine the left eigenvector $\mathbf{u}_1 = (0, 1)$ and the generalized eigenvector $\mathbf{u}_2 = (1, -w)$ consistent with orthonormalization conditions $\mathbf{u}_1\mathbf{v}_1 = 0$, $\mathbf{u}_1\mathbf{v}_2 = 1$, $\mathbf{u}_2\mathbf{v}_1 = 1$, and $\mathbf{u}_2\mathbf{v}_2 = 0$. One can directly verify that a kind of completeness condition $\mathbf{v}_1 \otimes \mathbf{u}_2 + \mathbf{v}_2 \otimes \mathbf{u}_1 = I_2$ holds true.

1.2.4 Symmetry and the EP order

The EP of the rth order emerges, when r eigenvalues become equal. The order of the EP is limited not only by dimensionality n of the system of equations (1.1), but also by the number of parameters. Suppose we have the EP of the rth order and m parameters $\vec{\alpha} = (\alpha_1, \ldots, \alpha_m)^T$. Then we have $r - 1$ equations $\lambda_1(\vec{\alpha}_0) = \lambda_2(\vec{\alpha}_0), \ldots, \lambda_1(\vec{\alpha}_0) = \lambda_r(\vec{\alpha}_0)$ for real (imaginary) eigenvalues, which can be consistently satisfied only if the number of equations is not greater than the number of parameters, i.e., $r - 1 \leq m$. The statement that the order of the EP is limited by the number of parameters as $r \leq m + 1$ is similar to the Gibbs phase rule for the systems in thermodynamic equilibrium. In the case of a single parameter α, $m = 1$ and the maximal order of the EP is $r = 2$ even if $n > 2$. In the case of complex eigenvalues, the number of equations doubles and the order of the EP should be within the range $2 \leq r \leq m/2 + 1$. Thus, the EP can exist only if the number of parameters $m \geq 2$.

Since, generally (for the complex eigenvalues), the minimal number of parameters is $2(r-1)$ for the r-th order EP, one should simultaneously tune $2(r-1)$ parameters that might be inconvenient and hardly realizable in practice. If the system satisfies some symmetries, the parameter space can be significantly reduced [15,16]. The most popular symmetries are parity ($\mathcal{P}$), parity–time ($\mathcal{PT}$), and charge-conjugation–parity ($\mathcal{CP}$) ones able to decrease the number of tuned parameters to $r - 1$ [16]. For example, for the second order EP one has to tune a single parameter instead of two parameters. The higher-order EPs can be realized due to increasing the number of channels in the system. In the optical context, this means that one should increase the number of coupled waveguides or cavities [17,18] or excite additional modes [19]. The order of EPs can be also doubled in the system consisting of two subsystems with identical degenerate eigenvalues. In this case, the merger of two individual EPs occurs only if the unidirectional coupling takes place [20].

Symmetric non-Hermitian Hamiltonians attract particular attention, because they can also provide a real spectrum of eigenvalues. If the symmetry is described by the linear operator $\hat{S}$, then it should commute with a symmetric Hamiltonian as $[\hat{H}, \hat{S}] = \hat{H}\hat{S} - \hat{S}\hat{H} = 0$. In the case of an anti-symmetric Hamiltonian, one should write the anti-commutation relation, $\{\hat{H}, \hat{S}\} = \hat{H}\hat{S} + \hat{S}\hat{H} = 0$.

One of the most studied symmetries is the parity–time ($\mathcal{PT}$) symmetry $\hat{S} = \hat{P}\hat{T}$, where $\hat{P}$ and $\hat{T}$ are the parity and time operators, respectively. The parity operator inverts spatial coordinates $\mathbf{r} \to -\mathbf{r}$. The time operator reverses time $t \to -t$, what is equivalent to the complex conjugate. The $\mathcal{PT}$-symmetric

Hamiltonian $\hat{H}(\mathbf{r},t)$ satisfies the commutation condition $\hat{P}\hat{T}\hat{H}(\mathbf{r},t)\psi(\mathbf{r},t) = \hat{H}(\mathbf{r},t)\hat{P}\hat{T}\psi(\mathbf{r},t)$ for an arbitrary wave function $\psi(\mathbf{r},t)$. Since operators $\hat{P}$ and $\hat{T}$ act on the right-standing quantities, we arrive at $\hat{H}(-\mathbf{r},-t)\psi(-\mathbf{r},-t) = \hat{H}(\mathbf{r},t)\psi(-\mathbf{r},-t)$. Excluding arbitrary wave function ψ, we conclude that the Hamiltonian is $\mathcal{PT}$-symmetric, if $\hat{H}(-\mathbf{r},-t) = \hat{H}(\mathbf{r},t)$. For time-independent Hamiltonians, this condition reads $\hat{H}^*(-\mathbf{r}) = \hat{H}(\mathbf{r})$. For a quantum particle in potential $V(\mathbf{r})$, the condition of $\mathcal{PT}$ symmetry is valid, when $V^*(-\mathbf{r}) = V(\mathbf{r})$. The Maxwell equations can be recast in the form of the Schrödinger equation (1.1) with the Hamiltonian

$$H(\mathbf{r}) = \begin{pmatrix} 0 & -i\mu^{-1}(\mathbf{r})\nabla\times \\ i\varepsilon^{-1}(\mathbf{r})\nabla\times & 0 \end{pmatrix}, \tag{1.30}$$

$\tau = ct$, and the wave function $\psi(\mathbf{r},t) = (\mathbf{H}(\mathbf{r},t), \mathbf{E}(\mathbf{r},t))^T$. Here $\mathbf{H}$ and $\mathbf{E}$ are the magnetic and electric field strengths and ε and μ are the permittivity and permeability tensors, respectively. $\mathcal{PT}$ symmetry then demands spatial distribution of material parameters according to $\varepsilon(\mathbf{r}) = \varepsilon^*(-\mathbf{r})$ and $\mu(\mathbf{r}) = \mu^*(-\mathbf{r})$, i.e., the permittivity and permeability play similar role as the potential in the context of quantum mechanics. Practical realization of the optical $\mathcal{PT}$ symmetry imposes severe restrictions on the choice of materials with gain and loss. To relax these requirements, an approach of the gain-free $\mathcal{PT}$ symmetry for input evanescent electromagnetic waves is proposed in Ref. [21].

Using the Fourier sum, a wave function in the box $L\times L\times L$ can be decomposed over countable number of orthogonal functions $f_{\mathbf{k}} = L^{-3/2}\exp(i\mathbf{kr})$ as $\psi(\mathbf{r}) = \sum_{\mathbf{k}}\psi_{\mathbf{k}}f_{\mathbf{k}}$. Then the wave function in the basis $\{f_{\mathbf{k}}\}$ can be presented as a vector $\psi = (\psi_{\mathbf{k}_n}, \psi_{\mathbf{k}_{n-1}}, \ldots, \psi_{-\mathbf{k}_n})^T$, where n is any integer number including infinity. From two expressions $\psi(-\mathbf{r}) = \hat{P}\psi(\mathbf{r})$ and $\psi(-\mathbf{r}) = \sum_{\mathbf{k}}\psi_{\mathbf{k}}f_{-\mathbf{k}} = \sum_{\mathbf{k}}\psi_{-\mathbf{k}}f_{\mathbf{k}}$ we can define the parity operator $\hat{P}$ as a matrix that should exchange the components $\psi_{\mathbf{k}_m}$ and $\psi_{-\mathbf{k}_m}$ of the wave function. That is why the parity operator for the two-state Hamiltonian reads

$$\hat{P} = \begin{pmatrix} 0 & 1 \\ 1 & 0 \end{pmatrix}. \tag{1.31}$$

The $\mathcal{PT}$-symmetric two-state Hamiltonian satisfies $\hat{P}\hat{T}\hat{H}\psi = \hat{H}\hat{P}\hat{T}\psi$, or $\hat{P}\hat{H}^*\psi^* = \hat{H}\hat{P}\psi^*$ for any wave function ψ. Therefore, $\hat{P}\hat{H}^* = \hat{H}\hat{P}$. For the two-dimensional matrices $\hat{P}$ and $\hat{H}$, $\mathcal{PT}$-symmetry imposes the restrictions on the Hamiltonian matrix elements as $H_{12} = H_{21}^*$ and $H_{11} = H_{22}^*$. The invariants $\mathrm{tr}(\hat{H}) = 2\mathrm{Re}(H_{11})$ and $\det(\hat{H}) = |H_{11}|^2 - |H_{12}|^2$ appear to be real-valued as well as the eigenvalues of the non-Hermitian Hamiltonian shown in Fig. 1.3.

Anti-$\mathcal{PT}$ symmetry arises, when $\hat{P}\hat{T}\hat{H} = -\hat{H}\hat{P}\hat{T}$. For the two-state Hamiltonian, we have $\hat{P}\hat{H}^* = -\hat{H}\hat{P}$, so that the matrix elements are $H_{12} = -H_{21}^*$ and $H_{11} = -H_{22}^*$. This drastically changes the invariants of the matrix $\hat{H}$: $\mathrm{tr}(\hat{H}) = 2i\mathrm{Im}(H_{11})$ and $\det(\hat{H}) = |H_{12}|^2 - |H_{11}|^2$. The eigenvalues are no longer real, but the EP still exists at $\det(\hat{H}) = (\mathrm{tr}(\hat{H}))^2/4$ as demonstrated for a generic system in Fig. 1.2.

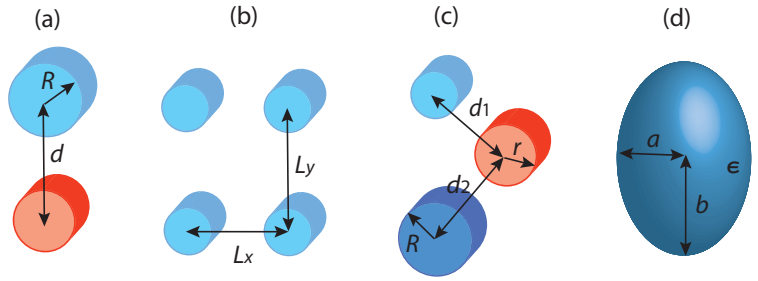

FIGURE 1.4 Types of resonators lacking a symmetry with the possible parameters for tuning. (a) Two cylinders, (b) two-dimensional array of cylinders, (c) three cylinders, and (d) spheroidal particle.

Although the discussion in this section concerns the EPs in the spectra of Hamiltonians, the similar regularities hold true for other matrices describing physical systems, too. One of such matrices is the scattering matrix widely used in photonics. In particular, the scattering matrix is highly convenient for the analysis of optical multilayer structures. The study of EPs using scattering matrices can be found in many publications, see, e.g., Refs. [22,23].

1.3 EXCEPTIONAL POINTS IN ISOLATED AND COUPLED DIELECTRIC RESONATORS

We start discussion of specific realizations of exceptional points with the photonic systems consisting of ordinary dielectric materials. Although non-Hermitian effects are usually associated with the presence of loss and gain, the non-Hermiticity can be provided solely by the radiative energy exchange with environment, without intrinsic absorption or amplification of radiation. In general, the eigenvalues (frequencies or wavevectors of the eigenmodes) remain complex even at the EP due to uncompensated radiative losses.

One of the first examples of the EPs in such all-dielectric structures was reported in Ref. [24]. The authors considered a pair of infinitely-long circular waveguides of different radii. In accordance with the discussion above, the lack of symmetry in such a system implies that one has to tune two independent parameters in order to reach the EP of the second order in the complex plane. For the two cylinders, one can use the radius of one of the cylinders (another has a fixed radius) and the distance between them as the tuned parameters [Fig. 1.4(a)]. For the rectangular lattice of four identical cylinders, it is convenient to exploit the distances between the cylinders in two orthogonal directions [Fig. 1.4(b)]. The third-order EP can be found in the system of three different cylinders by tuning four independent parameters, for example, two radii (eigenfrequencies of resonators) and two distances between the cylinders (coupling coefficients) [Fig. 1.4(c)].

It was shown further that a single dielectric resonator is enough to observe the EP, if it has an asymmetric (non-spherical) shape. For example, in the dielectric spheroidal particle [Fig. 1.4(d)], the EP can be caught in tuning the permittivity of the material and the aspect ratio of the radii along two orthogonal axes [25]. The same reasoning is true for the dielectric disc with the permittivity and the thickness-to-radius ratio as the parameters [26]. A system of dimers composed of discs can be more practical for observation of the EPs, because distances between the dimers and between the separate discs in the dimers are the parameters allowing easier control [26]. Note that in all cases mentioned above, the quality (Q) factor is strongly enhanced at the EP, what is important for various applications.

It seems that introduction of the asymmetry or deformation is the general method for reaching EPs in dielectric resonators caused by the control of modes evolution. As further examples, we mention the whispering-gallery modes cavities either having non-circular (quad-cosine [27] or limaçon [28]) shape or perturbed by additional scatterers [29].

1.4 EXCEPTIONAL POINTS IN NON-HERMITIAN SYSTEMS WITH GAIN AND LOSS

Although the non-Hermitian physics describes any open photonic system, it has been proved to be especially fruitful, when applied to active systems containing loss and gain components. Perhaps, the most intriguing class of such non-Hermitian systems possesses $\mathcal{PT}$ symmetry. The idea of the optical $\mathcal{PT}$ symmetry was adopted directly from quantum mechanics. In the pioneer work [30], it was shown that the $\mathcal{PT}$-symmetric Hamiltonian commuting simultaneously with the parity and time reversal operators have real eigenvalues. Since the stationary Schrödinger equation

$$\frac{d^2\psi}{dx^2} - \frac{2m}{\hbar^2}[V(x) - E] = 0 \tag{1.32}$$

for the quantum particle in the potential $V(x)$ is mathematically equivalent to the Helmholtz equation

$$\frac{d^2u}{dx^2} + \frac{\omega^2}{c^2}\varepsilon(x)u = 0 \tag{1.33}$$

for electromagnetic field in the medium with permittivity $\varepsilon(x)$, the transfer of $\mathcal{PT}$-symmetry to the optics domain is straightforward [5]. Obviously, the permittivity in optics plays the role of the potential in quantum mechanics. The $\mathcal{PT}$ symmetry condition for the potential $V(x) = V^*(-x)$ is then recast to $\varepsilon(x) = \varepsilon^*(-x)$. This means that $\mathcal{PT}$ symmetry can be realized in photonic structures with specific distributions of loss [$\mathrm{Im}(\varepsilon) > 0$] and gain [$\mathrm{Im}(\varepsilon) < 0$] over the media. The $\mathcal{PT}$-symmetric optical systems were realized using coupled waveguides [31,32], coupled cavities [33,34], and multilayer structures [35,36].

An EP in a $\mathcal{PT}$-symmetric photonic system can be defined as a point of spontaneous symmetry breaking. In other words, despite the condition $\varepsilon(x) = \varepsilon^*(-x)$ always holds true, the commutation of the Hamiltonian with the $\hat{P}$ and $\hat{T}$ operators is violated at the EP. One can introduce two phases touching at the EP: the first phase is $\mathcal{PT}$-symmetric with real eigenfrequencies and $\mathcal{PT}$-symmetric eigenmodes characterized by the balanced distribution of light energy over loss and gain components; the second phase is $\mathcal{PT}$-symmetry-broken with the complex eigenfrequencies and asymmetric eigenmodes demonstrating either strong amplification or attenuation of light. Exactly such a behavior of the modes is presented in Fig. 1.3. We should also emphasize that, as already discussed above, the $\mathcal{PT}$ symmetry diminishes the number of parameters needed for tuning the system towards the EP.

Let us consider the archetypal case of a loss-gain multilayer structure. Interaction of light with such non-Hermitian structures can be conveniently described with the scattering matrix formalism. The proper expression for the scattering matrix can be derived from the Hamiltonian similar to (1.30) and reads [23]

$$\hat{S} = \begin{pmatrix} t & r_R \\ r_L & t \end{pmatrix}, \tag{1.34}$$

where t, r_R, and r_L are the transmission and reflection coefficients which can be readily calculated with the well-known transfer matrix approach [37]. The eigenvalues of the matrix (1.34) are $s_{1,2} = t \pm \sqrt{r_R r_L}$, so that the EP corresponds to the situation when either r_R or r_L vanishes and $|t| = 1$ (Fig. 1.5). This is exactly the condition for the so-called anisotropic transmission resonances with the unitary transmission and the one-sided reflectionlessness [22]. If the multilayer structure is $\mathcal{PT}$-symmetric, i.e., consists of the balanced sequence of loss and gain layers, then the EP lies at the border between the $\mathcal{PT}$-symmetric phase with $|s_{1,2}| = 1$ and the $\mathcal{PT}$-symmetry-broken phase with $|s_1| = 1/|s_2| < 1$.

Another definition of the scattering matrix used in literature [22] reads as

$$\hat{S}' = \begin{pmatrix} r_L & t \\ t & r_R \end{pmatrix}. \tag{1.35}$$

The exchange of matrix elements in comparison to Eq. (1.34) may seem to be inessential, but actually it results in a dramatic change of the eigenvalues which now take the form $s'_{1,2} = (r_R + r_L)/2 \pm \sqrt{t^2 + (r_L - r_R)^2/4}$. The exceptional point also changes its position being observed at $|r_L + r_R| = 2$. Since $\hat{S}'$ does not follow from the $\mathcal{PT}$-symmetric Hamiltonian, the corresponding EP is not a true EP, but it is not meaningless as well. It makes sense as a lasing predictor showing the level of loss and gain just below the lasing threshold (Fig. 1.5). This interpretation was proved with the calculations based on the Maxwell-Bloch equations for realistic loss and gain media [23]. The Maxwell-Bloch approach as opposed to the usual phenomenological consideration based on complex permittivity allows taking nonlinear saturation into account and describing behavior in the lasing regime

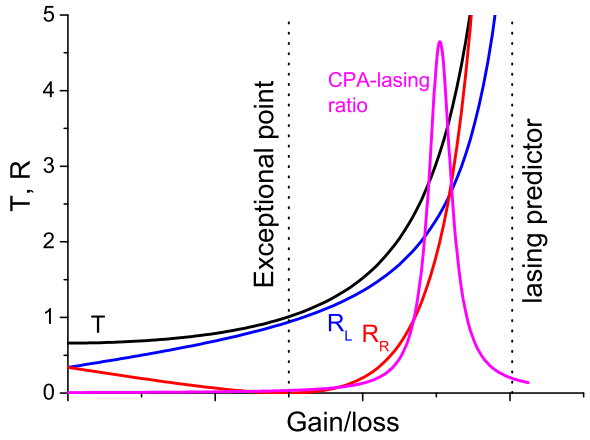

FIGURE 1.5 The EP of a $\mathcal{PT}$-symmetric multilayer structure. The EP corresponds to the unity transmission and zero reflection from one side. The lasing predictor corresponds to sharp increase of reflection and transmission. The ratio of output power in the cases corresponding to lasing and CPA reaches maximum between the EP and lasing predictor.

with the intriguing propagation locking effect [38]. It should be also noted that the EP as a lasing prethreshold was discussed in Ref. [39].

$\mathcal{PT}$ symmetry in photonic systems imposes tough limitations on loss and gain distribution raising a question of practical realization. That is why the non-Hermitian systems possessing EPs with relaxed demands on loss and gain are of extreme interest. As an example, we can spotlight anti-$\mathcal{PT}$-symmetric systems. In one-dimensional case, the anti-$\mathcal{PT}$-symmetry implies the permittivity of the form $\varepsilon(x) = -\varepsilon^*(-x)$. Since the imaginary part of the permittivity is either positive or negative in the entire space, the variety of passive materials can be employed in practice. However, this platform has a noticeable flaw preventing from the real-life application: it requires the utilization of exotic negative-refractive-index media [40]. More popular approach is based on the dissipative coupling of optical elements such as waveguides or cavities [41]. The dissipative coupling brings us to the special form of the Hamiltonian matrix that has real frequencies on the diagonal and complex coupling coefficients off the diagonal. The EPs in such anti-$\mathcal{PT}$-symmetric systems behave in the same way as for $\mathcal{PT}$-symmetric systems demarcating symmetric and symmetry-broken phases. The anti-$\mathcal{PT}$-symmetric EPs were reported in electric circuit resonators [42], optical fibers [43], and integrated-optics structures [44].

Passive analogue of the $\mathcal{PT}$-symmetric system is a promising paradigm for getting around the gain issues. Absorption modulation may emulate the true $\mathcal{PT}$ symmetry, if a constant shift of permittivities of all components in the system is made [5]. In this case, the less absorbing parts of the structure play the role of gain, whereas the more absorbing parts can be considered as loss.

In other words, the Hamiltonian matrix can be treated as a sum of the constant matrix and $\mathcal{PT}$-symmetric one. However, dissipative systems are dramatically different from those with balanced loss and gain, since the EPs are not necessary for $\mathcal{PT}$-symmetry-breaking transitions anymore [45]. A curious design of the passive $\mathcal{PT}$-symmetric structure is proposed in Ref. [46], where a mirror image supplements a passive structure instead of the real gain.

The unique features of EPs turned out to be extremely relevant for lasing as one of the typical non-Hermitian phenomena justified for the new class of $\mathcal{PT}$-symmetric lasers [47]. When the $\mathcal{PT}$ symmetry breaking at the EP violates balance between the modes, one of the modes becomes amplified and the other is attenuated. As a result, above the EP, which in this case is simultaneously the lasing threshold, the robust single-mode lasing is established. This idea being of high demand for applications was experimentally demonstrated with the microring lasers [48,49]. If the EP is above the lasing threshold, additional intriguing features emerge. For instance, the laser is able to turn off at the EP due to the coalescence of attenuating and amplifying modes [50,51]. The EP was predicted to be an on-off switching point also in the anti-$\mathcal{PT}$-symmetric lasing systems [52].

Sometimes a $\mathcal{PT}$-symmetric system can be simultaneously a coherent perfect absorber (CPA) and a laser. The CPA can be also called a time-reversed laser, or anti-laser, in the sense that incoming waves are fully absorbed in the medium due to their interference [53]. The CPA-lasing effect in $\mathcal{PT}$-symmetric systems was theoretically predicted in Ref. [54]. It shows up in the scenario of two counter-propagating waves impinging the system that behaves as a CPA or a laser depending on the phase difference between the waves [36]. The CPA-lasing conditions are not directly connected with emergence of the EPs. However, the optimal contrast between absorption and amplification appears to be reached above the EP, but below the lasing predictor point, as it was shown for multilayer structures (Fig. 1.5) [55]. This result supported by the time-domain Maxwell-Bloch simulations means that the CPA-lasing does not imply true lasing, because the latter is independent of the phase difference between the input waves [55].

1.5 TOPOLOGICAL PROPERTIES OF EXCEPTIONAL POINTS

Topology studies invariant, persistent properties of objects. These properties remain intact under perturbations or deformations of the object. The topological ideas penetrated first into condensed-matter physics being fruitful for explaining the features of quantum Hall effect and topological insulators. They proved to be extremely beneficial for description of optical systems (especially periodic, such as photonic crystals and metamaterials) giving rise to the field of topological photonics [56–58]. The key parameter characterizing the system from the viewpoint of topology is the topological invariant. Perhaps, the most widely used invariant is the Chern number which is the integral characteristic expressing the properties of the band structure of a complex photonic system in just one integer

[59].

Not pretending to cover all aspects of topological non-Hermitian systems [60,61], we limit our discussion to the specific problem of topological properties of EPs. The topology of any singular point including the EP can be characterized by the phase change under encircling this point in the parameter (or phase) space. The phase change under the closed path around the singular point defines the winding number

$$q = \frac{1}{2\pi} \oint d\phi. \tag{1.36}$$

The winding number q has the meaning of the topological charge of the singular point, the point being topologically nontrivial, if $q \neq 0$.

The topology of EPs is governed by geometry of the Riemannian surfaces formed by eigenvalues in the parameter space. An example of the Riemannian surfaces for the second-order EP is shown in Fig. 1.2. One can note that a single closed loop is not enough to return to the starting point on these surfaces and the second loop is needed. In this case, the EP's topological charge is $q = 1/2$, in contrast to the integer winding numbers in the topological systems supporting edge states. For the rth-order EP, one has r Riemannian surfaces and needs r loops to return to the starting point.

Moreover, the result of encircling the EP depends on the way it is performed. There are static and dynamic approaches to encircle the EP. For static encircling, the eigenmode swaps with another one at the different Riemannian surface gaining an additional (geometric) phase after returning to the starting point [62]. This is a direct consequence of the half-integer topological charge of the EP and the geometry of the Riemannian surfaces discussed above, so that the system does not return to the initial state in the end of the cycle. Perhaps, the first experimental observation of such a topological behavior was reported in 2001 for the two coupled microwave cavities perturbed by the semicircle scatterer [63]. Changing the position of the scatterer and coupling between the cavities, one can encircle the EP in the two-dimensional parameter space. The authors clearly observed the interchange of eigenvalues (complex frequencies) and eigenmodes (field distributions, see Fig. 1.6(a)) at the final point of the circle [63]. The swap of the eigenvalues was reported also for the coupled waveguides with purely radiative losses (see Section 1.3), including the case of higher-order EPs with multiple participating eigenmodes [24]. Static encircling the EP was also realized for the deformed optical microcavity [64] and the exciton-polariton microcavity of changing dimensions [65].

Totally different situation occurs for dynamic encircling when the measurements for the successive values of parameters are not independent. Changing characteristics of the system (e.g., its geometrical parameters or coupling strength with the environment) along the propagation direction provides the means to emulate the EP encircling in the parameter space. In this case, the process turns out to be non-adiabatic allowing jumps between the Riemannian surfaces [66,67]. Non-adiabaticity yields the chiral mode switching, when the final state depends

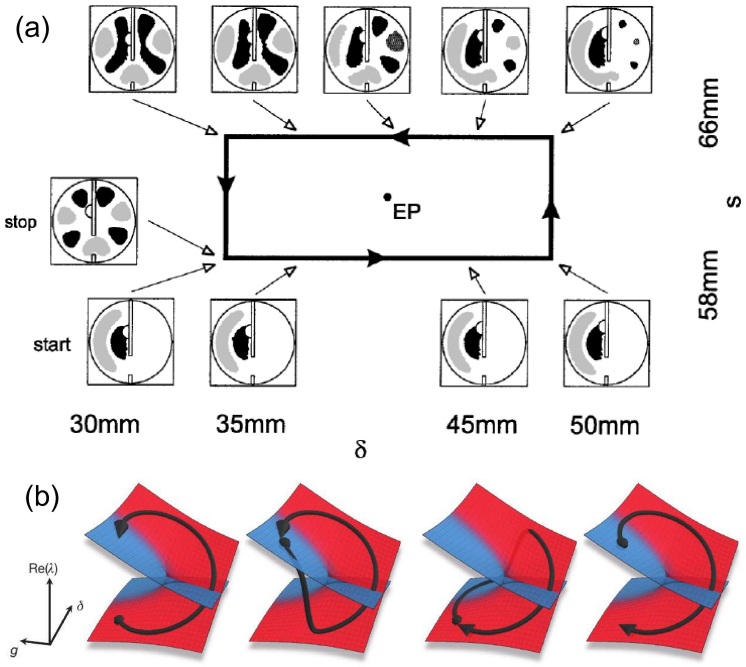

FIGURE 1.6 Topological features of the EPs. (a) Change of the field distribution for static encircling the EP. Adapted with permission from Ref. [63]. (b) Final state of a system depends on dynamic encircling direction (counter-clockwise for the two left panels, clockwise for the two right panels), but not on the starting point. Non-adiabatic jumps between the surfaces are clearly seen. Adapted with permission from Ref. [68].

on the encircling direction (clockwise or counter-clockwise), see Fig. 1.6(b). This effect was experimentally observed as an asymmetric light propagation in curved microwave waveguides [68] and in coupled photonic waveguides [69]. Dynamic effect of the moving EP and its encircling by the pair of waveguides was realized in Ref. [70]. Interestingly, the chiral mode switching is possible even if the loop does not encircle the EP itself, but is only situated nearby sensing the details of Riemannian surfaces [71,72]. In the case of multiple EPs, the dynamics of encircling become even richer, since the loops with the common starting points and encircling direction are not always topologically equivalent (homotopic) [73]. The multiple EP encircling was experimentally observed in the non-Hermitian waveguide arrays fabricated in glass [74].

In the presence of symmetries (for example, $\mathcal{PT}$ symmetry) additional features of encircling dynamics can be highlighted. In particular, the chirality of the dynamics remarkably depends on the starting point of encircling. If the starting point in the parameter space corresponds to the symmetric phase, the chiral switching depends on the encircling direction. To the contrary, the dynamics

are nonchiral (that is the final state is the same for any direction of encircling), if the starting point is in the broken-symmetry phase. A pronounced role of the starting point was demonstrated using a system of coupled waveguides made of ferromagnetic material well controlled by magnetic field [75]. The chiral switching in anti-$\mathcal{PT}$-symmetric systems was reported in Ref. [76].

The chiral mode switching is able to control the state of radiation polarization. It helps to design an optical omnipolarizer converting any input polarization into the desired one [77]. One more type of the chiral polarizer performed on the basis of anti-$\mathcal{PT}$-symmetric platform for waveguides was reported in Ref. [78].

1.6 ENHANCED SENSITIVITY AT THE EP

One of the most deeply studied and practically appealing effects observed in the EP vicinity is the sharp increase of system's sensitivity to an external perturbation. This effect allows using non-Hermitian systems as sensors to detect small changes of environment caused, e.g., by biomolecules. Enhanced sensitivity near the EP can be readily proved for the two-state Hamiltonian. Consider a non-Hermitian Hamiltonian $\hat{H}(\vec{\alpha}) = \hat{H}_0(\vec{\alpha}) + \varepsilon\hat{H}_1(\vec{\alpha})$, where $\varepsilon \ll 1$ is a dimensionless small parameter and $\varepsilon\hat{H}_1$ is a perturbation operator. The eigenvalues (1.23) of the non-perturbed system are degenerate at the EP, $\vec{\alpha} = \vec{\alpha}_0$, so that $f(0) = [\mathrm{tr}(\hat{H}_0)]^2 - 4\det(\hat{H}_0) = 0$, where $f(\varepsilon) = [\mathrm{tr}(\hat{H})]^2 - 4\det(\hat{H})$. When degeneracy is lifted due to the perturbation, the function takes the form $f(\varepsilon) \approx \varepsilon f'(0)$, where $f' = df/d\varepsilon$, and the eigenvalues (1.23) are equal to

$$\lambda_\pm = \frac{\mathrm{tr}(H_0) + \varepsilon\mathrm{tr}(\hat{H}_1) \pm \sqrt{\varepsilon f'(0)}}{2} \approx \lambda \pm \sqrt{\varepsilon}\frac{\sqrt{f'(0)}}{2}. \tag{1.37}$$

Square root of the small perturbation parameter is the leading order for the second-order EP. Owing to this fact, the sensitivity at the EP is enhanced in comparison to the usual situation of the linear relation between perturbation and response.

In general, the eigenvalues and eigenvectors can be presented as a Puiseux series in the EP vicinity:

$$\lambda_\pm = \sum_{k=0}^{\infty}(\pm 1)^k \varepsilon^{k/2}\lambda_k, \qquad \mathbf{v}_\pm = \sum_{k=0}^{\infty}(\pm 1)^k \varepsilon^{k/2}\tilde{\mathbf{v}}_k, \tag{1.38}$$

where λ_0 and $\tilde{\mathbf{v}}_0 = \mathbf{v}_1$ are the degenerate eigenvalues and eigenvectors at the EP, respectively. As shown in Ref. [79], in the leading order, the perturbed quantities can be written as $\lambda_\pm \approx \lambda_0 \pm \sqrt{\varepsilon}\lambda_1$, $\mathbf{v}_\pm \approx \mathbf{v}_1 \pm \sqrt{\varepsilon}\lambda_1\mathbf{v}_2$, and $\mathbf{u}_\pm \approx \mathbf{u}_1 \pm \sqrt{\varepsilon}\lambda_1\mathbf{u}_2$, where $\lambda_1 = \sqrt{(\mathbf{u}_1 H_1 \mathbf{v}_1)}$ and $\mathbf{v}_2$ ($\mathbf{u}_2$) is the right (left) generalized eigenvector. Adopting $(\mathbf{u}_1\mathbf{v}_2) = (\mathbf{u}_2\mathbf{v}_1) = 1$, the above approximations in the EP vicinity after substitution to (1.9) bring us to the dyadic Green function at the EP

$$G_{EP} = \frac{\mathbf{v}_1 \otimes \mathbf{u}_1}{(\lambda - \lambda_0)^2} + \frac{\mathbf{v}_2 \otimes \mathbf{u}_1 + \mathbf{v}_1 \otimes \mathbf{u}_2}{\lambda - \lambda_0}. \tag{1.39}$$

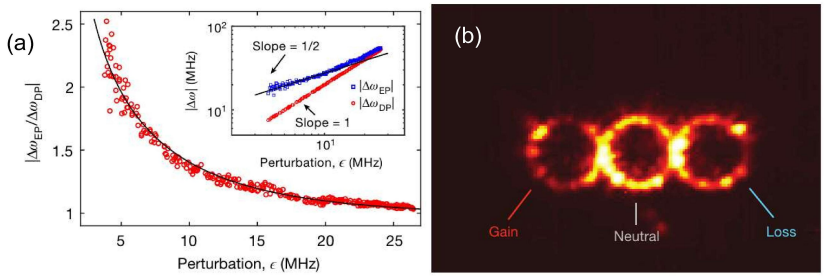

FIGURE 1.7 Sensing applications of the EPs. (a) Enhancement of the perturbation-induced frequency splitting of the cavity mode at the EP in comparison to the diabolic point (DP). Adapted with permission from Ref. [86]. (b) Intensity profile of the lasing mode at the 3rd order EP of the $\mathcal{PT}$-symmetric system consisting of three (loss, gain, and neutral) cavities. Adapted with permission from Ref. [87].

This equation is equivalent to the Green function at the EP in Eq. (1.22), because $\mathbf{v}_1 \otimes \mathbf{u}_1 = \hat{N}$ and $\mathbf{v}_1 \otimes \mathbf{u}_2 + \mathbf{v}_2 \otimes \mathbf{u}_1 = I_2$. Imaginary part of the Green function can be used to calculate the local density of states that behaves as the squared Lorentzian function being drastically different from the usual (non-degenerate) resonances and ensuring stronger response with narrower spectrum.

As for the rth-order EP, the leading order of the response is $\varepsilon^{1/r}$ [80]. Generally, the response strongly depends on the properties of perturbation Hamiltonian $\hat{H}_1$ and is proportional to $\varepsilon^{k/r}$, where k is an integer number up to r. For details, a reader is referred to literature on the perturbation theory near EPs [81–83].

Let us illustrate the general features discussed above with several specific examples. First of all, we should mention the idea of single-particle detection proposed and substantiated in Refs. [84,85]. The enhanced sensitivity at the EP for the single-particle detection in comparison to the Hermitian degeneracy at the diabolic point was experimentally demonstrated using the microtoroid whispering-gallery-mode cavity, see Fig. 1.7(a) [86]. Coupled loss-gain microring cavities were reported to provide thermal sensing [87]. $\mathcal{PT}$-symmetric system with the gain, loss, and neutral cavities demonstrated in Fig. 1.7(b) exhibits the cubic-root sensitivity to perturbation at the third-order EP [87]. Anti-$\mathcal{PT}$-symmetric scheme based on cavity-waveguide coupling was realized in Ref. [88] for detecting weak effect of mode anharmonicity. The EP-ehanced sensing proved to be especially useful for detecting rotations. The non-Hermitian gyroscopes exploiting the stimulated Brillouin scattering in the microresonator [89] and the ring laser [90] were reported to enhance the Sagnac effect. The anti-$\mathcal{PT}$-symmetric gyroscopes can be advantageous compared to the $\mathcal{PT}$-symmetric ones in accuracy and ease of realization [91,92]. The most exotic proposal being of fundamental importance is the search for the hypothetical axions using the $\mathcal{PT}$-symmetry-improved sensors [93,94].

We should note that the term “sensitivity” is used here to characterize the

connection between the perturbation (input) and the response (output). However, this does not guarantee the enhanced signal-to-noise ratio which is often more important for sensing applications. This fact has stirred up a discussion on the role of noise (both classical and quantum) in the non-Hermitian sensing. For more information on these debates and examples of specific EP sensors, we refer a reader to the recent papers [95,96].

1.7 EPS AND STRONG COUPLING

Let us look at Fig. 1.3 once again and think about it from the other side. The real and imaginary parts of eigenvalues can be associated with the resonant frequencies and widths of the resonances, respectively. Then, for $\eta < 1$, we see a single resonance, which splits into two resonances at $\eta > 1$. Such a splitting (so-called Rabi splitting) is characteristic for the strong-coupling regime of light-matter interaction, when both radiation and matter cease to be independent entities and exist in the form of part-matter–part-light polaritons [97,98]. From this point of view, the EP is the point of transition between the weak- and strong-coupling regimes or transition from modes crossing (overlap) to anti-crossing (splitting). The parameter η can be interpreted as the strength of the light-matter interaction governed by system's parameters, such as distances between waveguides or cavities.

There is a number of reports on strong coupling in the non-Hermitian context making emphasis on behaviors in the EP vicinity. One of the first such reports has substantiated applicability of the $\mathcal{PT}$ symmetry to the polaritonic domain by considering coupling between photonic and excitonic modes, e.g., in a semiconductor-quantum-well structure [99]. The EP originates from merging the polaritonic modes at some level of pumping below the lasing threshold. Moreover, encircling the EP results in switching the content of polaritons from pure photon to pure exciton and vice versa that seems to be intriguing for controlling light-matter interaction [99]. Polaritons may also stem from the plasmon and phonon modes coupled in the structure containing graphene and polar dielectric [100]. The transition between the weak and strong coupling regimes in these systems was shown to be controllable simply with light's angle of incidence [100]. The strong coupling regime in the non-Hermitian context was experimentally realized due to interaction of excitons with either photons or plasmons. In the first case [101], the polaritons emerge due to the excitons in the semiconductor GaN coupled to the whispering-gallery modes of the hexagonal microcavity. In the second case [102], the excitons in the transition metal dichalcogenide (in particular, tungsten disulfide WS_2) monolayer were coupled to plasmons of the silver nanogroove to form the polaritonic non-Hermitian system. The magnon-photon coupling in the system composed of the nitrogen centers in diamond and waveguide resonator was studied in Ref. [103].

1.8 CONCLUSION

In this Chapter, we have outlined the range of issues essential for the area of non-Hermitian photonics with the particular emphasis on the physics at the exceptional points. We have limited our discussion to the most basic and general properties of EPs originating from the non-Hermitian nature of Hamiltonian. We have illustrated the physics of EPs with a variety of examples from the optics and photonics literature. For the sake of brevity and clarity, we intentionally left aside many advanced topics and generalizations, such as exceptional rings [104] and surfaces [105,106] to mention a few. Nevertheless, we strongly believe that this Chapter will be of interest for everyone (especially, for beginners) interested in the non-Hermitian physics and its photonic applications.

ACKNOWLEDGEMENT

A.V.N. was supported by the Belarusian Republican Foundation for Fundamental Research (Project No. F21ISR-003). D.V.N. is grateful to the State Program for Scientific Research "Photonics and Electronics for Innovations" (Task 1.5). General theory of exceptional points was supported by the Russian Science Foundation (Project No. 21-12-00383).

BIBLIOGRAPHY

[1] Y. Ashida, Z. Gong, M. Ueda, Non-Hermitian physics, Adv. Phys. 69 (2020) 249-435.

[2] N. Moiseyev, *Non-Hermitian Quantum Mechanics*, Cambridge University Press, Cambridge, 2011.

[3] C. M. Bender, *PT Symmetry in Quantum and Classical Physics*, World Scientific, Singapore, 2019.

[4] D. Christodoulides, J. Yang (Eds.), *Parity-time Symmetry and Its Applications*, Springer, 2018.

[5] A. A. Zyablovsky, A. P. Vinogradov, A. A. Pukhov, A. V. Dorofeenko, A. A. Lisyansky, $\mathcal{PT}$ symmetry in optics, Phys. Usp. 57 (2014) 1063-1082.

[6] L. Feng, R. El-Ganainy, L. Ge, Non-Hermitian photonics based on parity-time symmetry, Nat. Photon. 11 (2017) 752-762.

[7] R. El-Ganainy, K. G. Makris, M. Khajavikhan, Z. H. Musslimani, S. Rotter, D. N. Christodoulides, Non-Hermitian physics and $\mathcal{PT}$ symmetry, Nat. Phys. 13 (2018) 11-19.

[8] S. K. Özdemir, S. Rotter, F. Nori, L. Yang, Parity-time symmetry and exceptional points in photonics, Nat. Mater. 18 (2019) 783-798.

[9] M.-A. Miri, A. Alù, Exceptional points in optics and photonics, Science 363 (2019) eaar7709.

[10] A. Krasnok, N. Nefedkin, A. Alù, Parity-Time Symmetry and Exceptional Points, IEEE Ant. Prop. Mag. 63 (2021) 110-121.

[11] G. N. Borzdov, Waves with linear, quadratic and cubic coordinate dependence of amplitude in crystals, Pramana 46 (1996) 245-257.

[12] T. G. Mackay, C. Zhou, A. Lakhtakia, Dyakonov–Voigt surface waves, Proc. R. Soc. A 475 (2019) 20190317.

[13] W. D. Heiss, Green's Functions at Exceptional Points, Int. J. Theor. Phys. 54 (2015) 3954-3959.

[14] J. Wiersig, Response strengths of open systems at exceptional points, arXiv:2203.12920v1 (2022).

[15] I. Mandal, E. J. Bergholtz, Symmetry and Higher-Order Exceptional Points, Phys. Rev. Lett. 127 (2021) 186601.

[16] P. Delplace, T. Yoshida, Y. Hatsugai, Symmetry-Protected Multifold Exceptional Points and Their Topological Characterization, Phys. Rev. Lett. 127 (2021) 186602.

[17] X. Zhou, S. K. Gupta, Z. Huang, Z. Yan, P. Zhan, Z. Chen, M. Lu, Z. Wang, Optical lattices with higher-order exceptional points by non-Hermitian coupling, Appl. Phys. Lett. 113 (2018) 101108.

[18] S. M. Zhang, X. Z. Zhang, L. Jin, Z. Song, High-order exceptional points in supersymmetric arrays, Phys. Rev. A 101 (2020) 033820.

[19] A. V. Hlushchenko, D. V. Novitsky, V. I. Shcherbinin, V. R. Tuz, Multimode $\mathcal{PT}$-symmetry thresholds and third-order exceptional points in coupled dielectric waveguides with loss and gain, J. Opt. 23 (2021) 125002.

[20] Q. Zhong, J. Kou, K. Özdemir, R. El-Ganainy, Hierarchical Construction of Higher-Order Exceptional Points, Phys. Rev. Lett. 125 (2020) 203602.

[21] H. Li, A. Mekawy, A. Alù, Gain-Free Parity-Time Symmetry for Evanescent Fields, Phys. Rev. Lett. 127 (2021) 014301.

[22] L. Ge, Y. D. Chong, A. D. Stone, Conservation relations and anisotropic transmission resonances in one-dimensional $\mathcal{PT}$-symmetric photonic heterostructures, Phys. Rev. A 85 (2012) 023802.

[23] A. Novitsky, D. Lyakhov, D. Michels, A. A. Pavlov, A. S. Shalin, D. V. Novitsky, Unambiguous scattering matrix for non-Hermitian systems, Phys. Rev. A 101 (2020) 043834.

[24] A. Abdrabou, Y. Y. Lu, Exceptional points for resonant states on parallel circular dielectric cylinders, J. Opt. Soc. Am. B 36 (2019) 1659-1667.

[25] E. Bulgakov, K. Pichugin, A. Sadreev, Exceptional points in a dielectric spheroid, Phys. Rev. A 104 (2021) 053507.

[26] K. Pichugin, A. Sadreev, E. Bulgakov, Exceptional Points through Variation of Distances between Four Coaxial Dielectric Disks, Photonics 8 (2021) 460.

[27] T. Jiang, Y. Xiang, Perfectly-matched-layer method for optical modes in dielectric cavities, Phys. Rev. A 102 (2020) 053704.

[28] S.-J. Park, I. Kim, S. Rim, M. Choi, Chiral exceptional point in transformation cavity, Opt. Lett. 47 (2022) 1705-1708.

[29] S. Ramezanpour, A. Bogdanov, A. Alù, Y. Ra'di, Generalization of exceptional point conditions in perturbed coupled resonators, Phys. Rev. B 104 (2021) 205405.

[30] C. M. Bender, S. Boettcher, Real spectra in non-Hermitian Hamiltonians having $\mathcal{PT}$ symmetry, Phys. Rev. Lett. 80 (1998) 5243-5246.

[31] C. E. Rüter, K. G. Makris, R. El-Ganainy, D. N. Christodoulides, M. Segev, D. Kip, Observation of parity-time symmetry in optics, Nat. Phys. 6 (2010) 192-195.

[32] M. Kremer, T. Biesenthal, L. J. Maczewsky, M. Heinrich, R. Thomale, A. Szameit, Demonstration of a two-dimensional $\mathcal{PT}$-symmetric crystal, Nat. Commun. 10 (2019) 435.

[33] B. Peng, Ş. K. Özdemir, F. Lei, F. Monifi, M. Gianfreda, G. L. Long, S. Fan, F. Nori, C. M. Bender, L. Yang, Parity–time-symmetric whispering-gallery microcavities, Nat. Phys. 10 (2014) 394-398.

[34] L. Chang, X. Jiang, S. Hua, C. Yang, J. Wen, L. Jiang, G. Li, G. Wang, M. Xiao, Parity–time symmetry and variable optical isolation in active–passive-coupled microresonators, Nat. Photon. 8 (2014) 524-529.

[35] L. Feng, Y.-L. Xu, W. S. Fegadolli, M.-H. Lu, J. E. B. Oliveira, V. R. Almeida, Y.-F. Chen, A.

Scherer, Experimental demonstration of a unidirectional reflectionless parity-time metamaterial at optical frequencies, Nat. Mater. 12 (2013) 108-113.

[36] Z. J. Wong, Y.-L. Xu, J. Kim, K. O'Brien, Y. Wang, L. Feng, X. Zhang, Lasing and anti-lasing in a single cavity, Nat. Photon. 10 (2016) 796-801.

[37] M. Born, E. Wolf, *Principles of Optics*, 7th ed., Cambridge University Press, Cambridge, 1999.

[38] D. V. Novitsky, A. Karabchevsky, A. V. Lavrinenko, A. S. Shalin, A. V. Novitsky, $\mathcal{PT}$ symmetry breaking in multilayers with resonant loss and gain locks light propagation direction, Phys. Rev. B 98 (2018) 125102.

[39] A. A. Zyablovsky, I. V. Doronin, E. S. Andrianov, A. A. Pukhov, Yu. E. Lozovik, A. P. Vinogradov, A. A. Lisyansky, Exceptional Points as Lasing Prethresholds, Laser Photon. Rev. 15 (2021) 2000450.

[40] L. Ge, H. E. Türeci, Antisymmetric $\mathcal{PT}$-photonic structures with balanced positive- and negative-index materials, Phys. Rev. A 88 (2013) 053810.

[41] F. Yang, Y.-C. Liu, L. You, Anti-$\mathcal{PT}$ symmetry in dissipatively coupled optical systems, Phys. Rev. A 96 (2017) 053845.

[42] Y. Choi, C. Hahn, J. W. Yoon, S. H. Song, Observation of an anti-$\mathcal{PT}$-symmetric exceptional point and energy-difference conserving dynamics in electrical circuit resonators, Nat. Commun. 9 (2018) 2182.

[43] A. Bergman, R. Duggan, K. Sharma, M. Tur, A. Zadok, A. Alù, Observation of anti-parity-time-symmetry, phase transitions and exceptional points in an optical fibre, Nat. Commun. 12 (2021) 486.

[44] H. Fan, J. Chen, Z. Zhao, J. Wen, Y.-P. Huang, Antiparity-Time Symmetry in Passive Nanophotonics, ACS Photon. 7 (2020) 3035.

[45] Y. N. Joglekar, A. K. Harter, Passive parity-time-symmetry-breaking transitions without exceptional points in dissipative photonic systems, Photon. Res. 6 (2018) A51-A57.

[46] F. Yang, A. Hwang, C. Doiron, G. V. Naik, Non-Hermitian metasurfaces for the best of plasmonics and dielectrics, Opt. Mater. Express 11 (2021) 2326-2334.

[47] B. Qi, H.-Z. Chen, L. Ge, P. Berini, R.-M. Ma, Parity–Time Symmetry Synthetic Lasers: Physics and Devices, Adv. Opt. Mater. 7 (2019) 1900694.

[48] L. Feng, Z. J. Wong, R.-M. Ma, Y. Wang, X. Zhang, Single-mode laser by parity-time symmetry breaking, Science 346 (2014) 972-975.

[49] H. Hodaei, M.-A. Miri, M. Heinrich, D. N. Christodoulides, M. Khajavikhan, Parity-time–symmetric microring lasers, Science 346 (2014) 975-978.

[50] M. Liertzer, L. Ge, A. Cerjan, A. D. Stone, H. E. Türeci, S. Rotter, Pump-Induced Exceptional Points in Lasers, Phys. Rev. Lett. 108 (2012) 173901.

[51] M. Brandstetter, M. Liertzer, C. Deutsch, P. Klang, J. Schöberl, H. E. Türeci, G. Strasser, K. Unterrainer, S. Rotter, Reversing the pump dependence of a laser at an exceptional point, Nat. Commun. 5 (2014) 4034.

[52] Y. Duan, X. Zhang, Y. Ding, X. Ni, Single-cavity bi-color laser enabled by optical anti-parity-time symmetry, Photon. Res. 9 (2021) 1280-1288.

[53] Y. D. Chong, Li Ge, Hui Cao, A. D. Stone, Coherent Perfect Absorbers: Time-Reversed Lasers, Phys. Rev. Lett 105 (2010) 053901.

[54] S. Longhi, $\mathcal{PT}$-symmetric laser absorber, Phys. Rev. A 82 (2010) 031801(R).

[55] D. V. Novitsky, CPA-laser effect and exceptional points in $\mathcal{PT}$-symmetric multilayer structures, J. Opt. 21 (2019) 085101.

[56] L. Lu, J. D. Joannopoulos, M. Soljačić, Topological photonics, Nat. Photon. 8 (2014) 821-829.

[57] T. Ozawa, H. M. Price, A. Amo, N. Goldman, M. Hafezi, L. Lu, M. C. Rechtsman, D. Schuster, J. Simon, O. Zilberberg, I. Carusotto, Topological photonics, Rev. Mod. Phys. 91 (2019)

015006.
[58] G.-J. Tang, X.-T. He, F.-L. Shi, J.-W. Liu, X.-D. Chen, J.-W. Dong, Topological Photonic Crystals: Physics, Designs, and Applications, Laser Photon. Rev. 16 (2022) 2100300.
[59] D. Bisharat, R. Davis, Y. Zhou, P. Bandaru, D. Sievenpiper, Photonic Topological Insulators: A Beginner's Introduction, IEEE Ant. Prop. Mag. 63 (2021) 112-124.
[60] H. Wang, X. Zhang, J. Hua, D. Lei, M. Lu, Y. Chen, Topological physics of non-Hermitian optics and photonics: a review, J. Opt. 23 (2021) 123001.
[61] M. Parto, Y. G. N. Liu, B. Bahari, M. Khajavikhan, D. N. Christodoulides, Non-Hermitian and topological photonics: optics at an exceptional point, Nanophotonics 10 (2021) 403-423.
[62] A. A. Mailybaev, O. N. Kirillov, A. P. Seyranian, Geometric phase around exceptional points, Phys. Rev. A 72 (2005) 014104.
[63] C. Dembowski, H.-D. Gräf, H. L. Harney, A. Heine, W. D. Heiss, H. Rehfeld, A. Richter, Experimental Observation of the Topological Structure of Exceptional Points, Phys. Rev. Lett. 86 (2001) 787-790.
[64] S.-B. Lee, J. Yang, S. Moon, S.-Y. Lee, J.-B. Shim, S. W. Kim, J.-H. Lee, K. An, Observation of an Exceptional Point in a Chaotic Optical Microcavity, Phys. Rev. Lett. 103 (2009) 134101.
[65] T. Gao, E. Estrecho, K. Y. Bliokh, T. C. H. Liew, M. D. Fraser, S. Brodbeck, M. Kamp, C. Schneider, S. Höfling, Y. Yamamoto, F. Nori, Y. S. Kivshar, A. G. Truscott, R. G. Dall, E. A. Ostrovskaya, Observation of non-Hermitian degeneracies in a chaotic exciton-polariton billiard, Nature 526 (2015) 554-558.
[66] R. Uzdin, A. Mailybaev, N. Moiseyev, On the observability and asymmetry of adiabatic state flips generated by exceptional points, J. Phys. A 44 (2011) 435302.
[67] T. J. Milburn, J. Doppler, C. A. Holmes, S. Portolan, S. Rotter, P. Rabl, General description of quasiadiabatic dynamical phenomena near exceptional points, Phys. Rev. A 92 (2015) 052124.
[68] J. Doppler, A. A. Mailybaev, J. Böhm, U. Kuhl, A. Girschik, F. Libisch, T. J. Milburn, P. Rabl, N. Moiseyev, S. Rotter, Dynamically encircling an exceptional point for asymmetric mode switching, Nature 537 (2016) 76-79.
[69] J. W. Yoon, Y. Choi, C. Hahn, G. Kim, S. H. Song, K.-Y. Yang, J. Y. Lee, Y. Kim, C. S. Lee, J. K. Shin, H.-S. Lee, P. Berini, Time-asymmetric loop around an exceptional point over the full optical communications band, Nature 562 (2018) 86-90.
[70] Q. Liu, S. Li, B. Wang, S. Ke, C. Qin, K. Wang, W. Liu, D. Gao, P. Berini, P. Lu, Efficient Mode Transfer on a Compact Silicon Chip by Encircling Moving Exceptional Points, Phys. Rev. Lett. 124 (2020) 153903.
[71] A. U. Hassan, G. L. Galmiche, G. Harari, P. LiKamWa, M. Khajavikhan, M. Segev, D. N. Christodoulides, Chiral state conversion without encircling an exceptional point, Phys. Rev. A 96 (2017) 052129.
[72] H. Nasari, G. Lopez-Galmiche, H. E. Lopez-Aviles, A. Schumer, A. U. Hassan, Q. Zhong, S. Rotter, P. LiKamWa, D. N. Christodoulides, M. Khajavikhan, Chiral state conversion without encircling an exceptional point, Nature 605 (2022) 256-261.
[73] Q. Zhong, M. Khajavikhan, D. N. Christodoulides, R. El-Ganainy, Winding around non-Hermitian singularities, Nat. Commun. 9 (2018) 4808.
[74] F. Yu, X.-L. Zhang, Z.-N. Tian, Q.-D. Chen, H.-B Sun, General Rules Governing the Dynamical Encircling of an Arbitrary Number of Exceptional Points, Phys. Rev. Lett. 127 (2021) 253901.
[75] X.-L. Zhang, S. Wang, B. Hou, C. T. Chan, Dynamically Encircling Exceptional Points: In situ Control of Encircling Loops and the Role of the Starting Point, Phys. Rev. X 8 (2018) 021066.
[76] X.-L. Zhang, T. Jiang, C. T. Chan, Dynamically encircling an exceptional point in anti-parity-time symmetric systems: asymmetric mode switching for symmetry-broken modes, Light Sci. Appl. 8 (2019) 88.

[77] A. U. Hassan, B. Zneh, M. Soljačić, M. Khajavikhan, D. N. Christodoulides, Dynamically Encircling Exceptional Points: Exact Evolution and Polarization State Conversion, Phys. Rev. Lett. 118 (2017) 093002.

[78] Y. Wei, H. Zhou, Y. Chen, Y. Ding, J. Dong, X. Zhang, Anti-parity-time symmetry enabled on-chip chiral polarizer, Photon. Res. 10 (2022) 76-83.

[79] A. Pick, B. Zhen, O. D. Miller, C. W. Hsu, F. Hernandez, A. W. Rodriguez, M. Soljačić, S. G. Johnson, General theory of spontaneous emission near exceptional points, Opt. Express 25 (2017) 12325-12348.

[80] Y. Wu, P. Zhou, T. Li, W. Wan, Y. Zou, High-order exceptional point based optical sensor, Opt. Express 29 (2021) 6080-6091.

[81] V. Lidskii, Perturbation theory of non-conjugate operators, USSR Comp. Math. Math. Phys. 6 (1966) 73-85.

[82] J. Moro, J. V. Burke, M. L. Overton, On the Lidskii-Vishnik-Lyusternik perturbation theory for eigenvalues of matrices with arbitrary Jordan structure, SIAM J. Matrix Anal. Appl. 18 (1997) 793-817.

[83] Y. Ma, A. Edelman, Nongeneric eigenvalue perturbations of Jordan blocks, Linear Algebra and Its Applications 273 (1998) 45-63.

[84] J. Wiersig, Enhancing the Sensitivity of Frequency and Energy Splitting Detection by Using Exceptional Points: Application to Microcavity Sensors for Single-Particle Detection, Phys. Rev. Lett. 112 (2014) 203901.

[85] J. Wiersig, Sensors operating at exceptional points: General theory, Phys. Rev. A 93 (2016) 033809.

[86] W. Chen, Ş. K. Özdemir, G. Zhao, J. Wiersig, L. Yang, Exceptional points enhance sensing in an optical microcavity, Nature 548 (2017) 192-196.

[87] H. Hodaei, A. U. Hassan, S. Wittek, H. Garcia-Gracia, R. El-Ganainy, D. N. Christodoulides, M. Khajavikhan, Enhanced sensitivity at higher-order exceptional points, Nature 548 (2017) 187-191.

[88] J. M. P. Nair, D. Mukhopadhyay, G. S. Agarwal, Enhanced Sensing of Weak Anharmonicities through Coherences in Dissipatively Coupled Anti-PT Symmetric Systems, Phys. Rev. Lett. 126 (2021) 180401.

[89] Y.-H. Lai, Y.-K. Lu, M.-G. Suh, Z. Yuan, K. Vahala, Observation of the exceptional-point-enhanced Sagnac effect, Nature 576 (2019) 65-69.

[90] M. P. Hokmabadi, A. Schumer, D. N. Christodoulides, M. Khajavikhan, Non-Hermitian ring laser gyroscopes with enhanced Sagnac sensitivity, Nature 576 (2019) 70-74.

[91] M. De Carlo, F. De Leonardis, L. Lamberti, V. M. N. Passaro, High-sensitivity real-splitting anti-$\mathcal{PT}$-symmetric microscale optical gyroscope, Opt. Lett. 44 (2019) 3956-3959.

[92] H. Qin, Y. Yin, M. Ding, Sensing and Induced Transparency with a Synthetic Anti-$\mathcal{PT}$ Symmetric Optical Resonator, ACS Omega 6 (2021) 5463-5470.

[93] X. Li, M. Goryachev, Y. Ma, M. Tobar, C. Zhao, R. X. Adhikari, Y. Chen, Broadband sensitivity improvement via coherent quantum feedback with $\mathcal{PT}$-symmetry, Proc. SPIE 11700 (2021) 117002H.

[94] Y. Chen, M. Jiang, Y. Ma, J. Shu, Y. Yang, Axion haloscope array with $\mathcal{PT}$ symmetry, Phys. Rev. Research 4 (2022) 023015.

[95] J. Wiersig, Review of exceptional point-based sensors, Photon. Res. 8 (2020) 1457-1467.

[96] R. Duggan, S. A. Mann, and A. Alù, Limitations of Sensing at an Exceptional Point, ACS Photon. 10.1021/acsphotonics.1c01535 (2022).

[97] F. J. Garcia-Vidal, C. Ciuti, T. W. Ebbesen, Manipulating matter by strong coupling to vacuum fields, Science 373 (2021) eabd0336.

[98] D. G. Baranov, M. Wersäll, J. Cuadra, T. J. Antosiewicz, T. Shegai, Novel Nanostructures and Materials for Strong Light–Matter Interactions, ACS Photon. 5 (2018) 24-42.

[99] J. B. Khurgin, Exceptional points in polaritonic cavities and subthreshold Fabry–Perot lasers, Optica 7 (2020) 1015-1023.

[100] S. H. Park, S. Xia, S.-H. Oh, P. Avouris, T. Low, Accessing the Exceptional Points in a Graphene Plasmon–Vibrational Mode Coupled System, ACS Photon. 8 (2021) 3241-3248.

[101] H. G. Song, M. Choi, K. Y. Woo, C. H. Park, Y.-H. Cho, Room-temperature polaritonic non-Hermitian system with single microcavity, Nat. Photon. 15 (2021) 582-587.

[102] Y. Sang, C.-Y. Wang, S. S. Raja, C.-W. Cheng, C.-T. Huang, C.-A. Chen, X.-Q. Zhang, H. Ahn, C.-K. Shih, Y.-H. Lee, J. Shi, S. Gwo, Tuning of Two-Dimensional Plasmon–Exciton Coupling in Full Parameter Space: A Polaritonic Non-Hermitian System, Nano Lett. 21 (2021) 2596-2602.

[103] G.-Q. Zhang, Z. Chen, D. Xu, N. Shammah, M. Liao, T.-F. Li, L. Tong, S.-Y. Zhu, F. Nori, J. Q. You, Exceptional Point and Cross-Relaxation Effect in a Hybrid Quantum System, PRX Quant. 2 (2021) 020307.

[104] B. Zhen, C. W. Hsu, Y. Igarashi, L. Lu, I. Kaminer, A. Pick, S.-L. Chua, J. D. Joannopoulos, M. Soljačić, Spawning rings of exceptional points out of Dirac cones, Nature 525 (2015) 354-358.

[105] Q. Zhong, J. Ren, M. Khajavikhan, D. N. Christodoulides, Ş. K. Özdemir, R. El-Ganainy, Sensing with Exceptional Surfaces in Order to Combine Sensitivity with Robustness, Phys. Rev. Lett. 122 (2019) 153902.

[106] G.-Q. Qin, R.-R. Xie, H. Zhang, Y.-Q. Hu, M. Wang, G.-Q. Li, H. Xu, F. Lei, D. Ruan, G.-L. Long, Experimental Realization of Sensitivity Enhancement and Suppression with Exceptional Surfaces, Laser Photon. Rev. 15 (2021) 2000569.